

ANISOTROPY OF SOURCE PARAMETERS FROM INDUCED MICROSEISMICITY

Peter Starzec¹, Michael Fehler², Roy Baria³, Hiroaki Niitsuma⁴

¹Chalmers University, Gothenburg, Sweden

²Los Alamos Seismic Research Center, Los Alamos National Laboratory, USA

³Socomine, Soultz-sous-Forêts, France

⁴Tohoku University, Sendai, Japan

Abstract

We applied geostatistical techniques to seismic data to examine the permeability in the vicinity of the GPK1 injection well at Soultz HDR geothermal site (Alsace, France). 2D spatial distributions of shear displacement at the source of microearthquakes induced by hydraulic fracturing were studied by means of both omnidirectional and directional variogram functions computed in several vertical planes. The variogram function is a method for analysing the spatial correlation of a variable. The variograms obtained for four vertical slices (zones) along the wellbore were compared with results from a spinner flow-log run during an injection test, which provides information about near-wellbore permeability. Clear variations in 2D variograms with orientation were associated with permeable zones. There are also distinct differences in variogram shape between low and high permeability zones. The proposed method of analysis, while qualitative, may be useful for determining the permeability at locations within the reservoir that are far from injection wells.

Background

The Hot Dry Rock Geothermal Energy (HDR) concept relies on the use of hydraulic fracturing to enhance rock mass permeability through the creation of fractures between injection and recovery wells drilled into otherwise impermeable rock. Based on studies carried out at the Los Alamos National Laboratory (USA) and Camborne School of Mines (UK) it was suggested that the cause of permeability enhancement is due to shear failure induced along naturally existing joints by elevated pore fluid pressures (Fehler, 1989; Jupe, 1990). Several techniques exist to discern structural details within the zone of locations of the induced microseismic events (Fehler et al., 1987; Jones & Stewart, 1997; Phillips et al., 1997). These methods rely on the locations of the event hypocenters to define features in the event cloud. Another approach is the use of fault-plane solutions (Fehler 1990), which provide information about both the structure and mechanism of shearing. Roff et al. (1996) used the ratio of P- to S-wave first arrival amplitudes at a given station as an indicator of earthquake focal mechanism to cluster events. They analysed the pattern of locations within the clusters and identified planes which were considered to be fractures within the reservoir. Phillips et al. (1997) performed precise relative relocations of events in the Fenton Hill, US reservoir by picking relative arrival times on events having similar waveforms. They found that events in many

clusters fall along clear planes that can also be considered to be fractures within the reservoir. However, the method of delineating planes within the seismicity pattern provide no information about the relative flow permeability along the planes or even whether or not the planes are actual flow paths.

The analysis of the displacement spectra of P- and S-waves radiated by induced seismic events gives information about seismic source parameters including seismic moment, magnitude, stress drop, shear displacement, and source radius (Brune, 1970). Methods for calculation of the source parameters of seismic events induced by hydraulic fracturing and their physical interpretation are presented by Fehler and Phillips (1989) and Jupe (1990). While the source parameters themselves may be unreliable estimations of the actual source process, their spatial variation within a hydraulically stimulated reservoir may provide useful information for understanding flow of fluids through the reservoir. In this paper we present a methodology for analysing the spatial variations in computed shear displacement. We compare the parameters characterizing the spatial variations with measured fluid flow variations and find a relation between flow paths and spatial variation in source parameters. We test the method on a large data set of induced seismic events that occurred during stimulation of the HDR reservoir at Soultz-sous-Forêts, France.

Approach

The main objective of this study is to test a hypothesis on whether or not there is a relationship between spatial distribution of shear displacement accompanying induced seismic events within a reservoir and spatial variations in permeability caused by elevated fluid pressure during injection. Due to roughness along a fracture plane, the enlargement in joint apertures that is caused by shear dilation during a seismic event is likely to be of the order of 10 % of the total shear displacement (Brown, 1995; Jupe, 1990) thus, we intuitively expect a correlation between changes in permeability during fluid injection and the pattern of the detected seismicity. Seismic waveforms collected at the Soultz-sous-Forêts HDR site during a hydraulic injection during September 1993 were analyzed. During this injection, a total of 25300m³ of water were injected into wellbore GPK1 and a total of 13000 seismic events that were caused by the injection were located. Source parameters were calculated by spectral analysis of waveforms of 6600 of the events. Figure 1 shows the locations of 450 events that occurred within 50 m of injection wellbore GPK1. The region surrounding the wellbore is broken by depth into four zones of thickness 60 m as illustrated in the Figure. Shear displacements for 450 events were calculated from available source spectra calculated by Jones (personal communication) using

$$D = \frac{M_o}{\mu \pi R^2} \quad (1)$$

where:

D - shear displacement

M_o - seismic moment

μ - compressibility modulus

R - source radius

(Aki & Richards, 1980). Evans (personal communication) analyzed data from spinner logs collected in borehole GPK-1 to determine relative permeability of the zone surrounding the wellbore. A spinner records the rate of flow along a borehole. When there are changes in flow rate caused by flow leaving the wellbore, the spinner log records a signal that can be interpreted to infer relative permeability of the zone in the vicinity of the wellbore. The region shown in Figure 1 was divided into four distinct zones each having an extent of 60 m in the North-South direction corresponding to sections of different near-wellbore permeability as follows:

1. Zone 1 (2900-2925 m) was the most conductive zone since it accounted for more than 40% of net well flow out of the wellbore.
2. Zone 2 (2925-2975 m) was least conductive (accepted about 10 % of the net flow).
3. Zone 3 (2975-3140 m) was of relatively high conductivity (30 % acceptance)
4. Zone 4 (3140-3250 m) with medium to low conductivity, accepted about 15 % of the net flow.

Our procedure for investigating the relationship between permeability and seismic activity is based on spatial analysis of the distribution of shear displacement accompanying each induced microearthquake. To characterize the degree of continuity of a variable (D in our case) within defined zones (slices), a variogram function was calculated as a measure of variability (Journel & Huijbregts, 1978; Isaaks & Srivastava, 1989). In 2D, the variogram function is defined by :

$$\gamma(h_x, h_y) = \frac{1}{2n} \sum [z(x, y) - z(x + h_x, y + h_y)]^2 \quad (2)$$

where:

h_x, h_y - distance between event locations in x- and y-direction, respectively

$z(x, y)$ - value of estimated shear displacement of event at (x, y)

n - number of pairs of seismic events located at a distance (h_x, h_y) from each other

We consider variations in only a vertical plane so x represents the horizontal direction and y the vertical direction.

The concept of spatial analysis has been successfully used for locating structural discontinuities like folding and faulting planes (Hohn, 1988), or for locating ore bodies in mineral exploration (Journel & Huijbregts, 1978). Three parameters used to quantify a variogram are the nugget, net sill, and range. The nugget is the value of the variogram at zero offset, e.g. $\gamma(0, 0)$. The nugget is extrapolated from values at non-zero offset by following the trend to zero offset. The net sill value is the difference between the amplitude of the variogram where it levels off at large offset and the nugget. The range a is the distance beyond which the value of the variogram is relatively constant. The range is a measure of the continuity of the variogram. Physically, the nugget is a measure of the fine-scale variation in the phenomenon

under study and it might be influenced by the quality of data sampling. Sill is a measure of the overall spatial variation of the parameter. Range tells us how "fast" the variograms function stabilises and is usually associated with the size and extension of the structural features that control the parameter being measured.

Relation between Spatial Distribution of Permeability and Flow Directions

Borehole logging investigations performed at Soultz (Bresee, 1991) indicated that permeable fractures are clumped within zones and have a preferred orientation in space (i.e. a certain strike and dip). Following the notion that shear displacements along seismic sources induced by fluid injection are associated with increases in fracture apertures and that seismic slip planes fall in some preferred range of orientations, we postulate that the spatial continuity of shear displacement should have a similar pattern to the spatial character of the increase in permeability. In other words we presume some relation between the spatial distribution of shear displacement and the locations of permeable zones within the reservoir. This is consistent with the conclusions of Barton et al (1995) that permeable fractures tend to be those that have high resolved shear stresses. Fractures with high resolved shear stresses are those that are most likely to slip.

To examine the relation between directions of flow and preferred orientations of flow permeability, we performed tracer modelling using the GMS (Groundwater Modelling System) software (Engineering Computer Graphics Laboratory, 1996). As a first step, the Modflow-package for aquifer modelling was run and we subsequently used the Mt3D-package for solute transport. In this simulation a conservative tracer (non-adsorptive) was injected into 2-D zones of varying spatial distributions of permeability. Zones of randomly oriented permeability as well as zones with preferential orientations of permeability were examined. Relative concentration of tracer vs. distance and time was calculated. For each permeability distribution pattern, a set of directional variograms of permeability (termed anisotropy map in geostatistical terminology) was compared to tracer concentration maps derived from the modelling. Figure 2 shows the results for a zone having a relatively uniform distribution of permeability having preferred orientation in the North-South direction. Figure 3 shows results for a zone with a distribution of permeability that is both random in amplitude and orientation. In the case where permeability was oriented predominantly in the N-S direction, the variogram function of permeability exhibited minimum variation (N-S azimuth on Figure 2a). For this case, the fluid flow directions determined from the flow modelling indicated a predominant N-S flow orientation (Figure 2b). For the case where a randomly oriented distribution of permeability was chosen, the variogram, Figure 3a, is far more indistinct and directions of maximum and minimum continuity are rather difficult to define. It is also more difficult to find prevailing flow directions from the modelling results, shown in Figure 3b. From the numerical simulations, we conclude that the more regular pattern of spatial distribution of permeability the more distinct are the flow directions. If seismic events induce a local increase of permeability due to shear slip and dilation, a predominant alignment of seismic sources is likely to cause a predominant alignment of flow direction.

Results

Analysis of variogram functions for shear displacement distribution for each zone identified in Figure 1 along borehole GPK1 was carried out. To simplify the interpretation, omnidirectional variograms (variograms independent of direction) rather than anisotropy maps for each zone were derived. In this case, a variogram is calculated as a function of offset, h , only rather than a function of separation along coordinate axes. Figure 4a-d present omnidirectional variograms calculated from the data for zones 1-4. In geostatistics, variograms are usually fit using portions of exponential functions, Gaussian functions or segments of spheres. For each candidate function, a best-fit model is found and the best fit among the three functions is chosen to characterize the variogram. Parameters characterizing the best-fit function are then used to estimate the nugget, sill, and range. For zone 1 (Figure 4a), we find that a function describing a portion of a sphere best fits the data. For zone 2, 3 and 4 (Figures 4b-d) the Gaussian function provides the best fit to the data. Table 1 lists the values determined for the nugget, sill, and range for each region.

Zones 1 and 3, Figure 4a, b, have almost zero nugget and have a relatively large net sill values. Those two zones have relatively high permeability and account for 40 % and 30 % respectively of the fluid acceptance based on spinner log analysis during the injection test. The other two zones, 4 and 2 (Figure 4c, d, respectively) have variogram shapes that differ from those of the more permeable zones. The nuggets for the less permeable zones are considerably larger and net sills have lower values than those of zones 1 and 3. Relatively little fluid enters the formation from zones 2 and 4, which account for 10 % and 15 % of the fluid flow. The variogram for zone 2 (Figure 4 d) reflects a spatial distribution pattern of shear displacement that is close to random, having a high nugget and almost constant $\gamma(h)$ implying the shear displacement pattern is independent of spatial location.

Systematic errors in locations may introduce some structure into the shape of a variogram; such errors may vary with position within the reservoir. We have no way to reliably characterize systematic location errors or their influences on the variogram shape. As a simple test of the influences of locations on variogram shapes, we randomly assigned one of the source slips determined for a given microearthquake to another event within the same zone. We then calculated variograms for this randomized data. For each of the four zones, we found that the variograms determined using the randomized slips were nearly flat indicating no correlation among randomized slip and event location. While this test does not place limits on the reliability of our reported variogram shapes, it does indicate that there is structure in the actual shear-displacement data that is not apparent in random data, and further that this structure is not caused by the microearthquake location pattern.

Another parameter distinguishing between permeable and relatively impermeable zones could be anisotropy ratio (A_z), defined by

$$A_z = a_1 / a_2 \quad (3)$$

where a_1 is a range of a variogram computed in a direction of maximum continuity, a_2 is a range of a variogram computed in a direction of minimum continuity. The directions of minimum and maximum continuity are usually orthogonal.

Equation (3) is valid only when variograms exhibit the same sill in all directions. Graphically, the anisotropy can be represented by an anisotropy ellipse, where the longer axis equals a_1 and the shorter axis equals a_2 (see Isaaks & Srivastava 1989). Both the anisotropy ratio A_z and the orientation (azimuth) of the anisotropy ellipse in space are important for interpretation of the angular variation of the parameter being investigated. Both a_1 and a_2 must be measured at a location where the variograms in the two directions have the same value. Thus, we arbitrarily choose a value of $\gamma(h)$ that is smaller than the sill; then for the chosen $\gamma(h)$ we find the corresponding h -values for both directions. Figure 5 shows how A_z for zone 3 was calculated. First the directions of maximum and minimum continuity were determined. We choose to work in a vertical plane so directions of minimum and maximum continuity vary from vertical to horizontal. For zone 3 the direction of maximum continuity was found to be $90 \pm 15^\circ$ (Figure 5a) where 0° corresponds to the horizontal direction. That means that in zone 3, the permeable fracture zone is almost vertical. The direction of minimum continuity was found to be $20 \pm 15^\circ$ and the variogram for zone 3 in this direction is shown in Figure 5b.

It was found that A_z for zones 1 and 3 are about twice as large as A_z for zones 4 and 2. This indicates that within zones of a higher fluid acceptance (higher average permeability), the prevailing fluid directions tend to be more oriented in a single direction whereas prevailing directions are less well defined in zones of lower fluid acceptance. Thus, zones of higher capacity to accept injected fluid reveal a clearer anisotropy pattern than zones of low permeability.

Conclusions

We have found a correlation between the characteristics of variograms of shear displacement accompanying induced seismic events and permeability of a near-wellbore region. There is a clear difference in the variograms between relatively permeable and impermeable zones. While this correlation has been found to hold in the vicinity of a borehole, it may be reasonable to extend it to remote regions in a reservoir where it is desirable to make some inferences about relative permeability. In that manner, shear displacement (or some other source parameter) could provide information on joint permeability and prevailing fluid directions. Since this approach may offer the opportunity to study the permeability distribution far from the wellbore, where other measurements cannot provide direct evidence of permeability, more investigation is needed to examine the reliability of the method.

Acknowledgements

We thank Rob Jones for providing the locations and results of spectral analysis of waveforms that formed the basis of this study. Keith Evans provided information about the flow characteristics and valuable feedback on the methods used in the analysis presented here. We wish to thank Scott Phillips and Reinhard Jung for valuable discussion and consultation.

Jim Rutledge read the manuscript and gave us several valuable suggestions for its improvement. The work of Peter Starzec was funded by the European Commission as part of their Hot Dry Rock Geothermal Project. This work was performed as part of the MTC (More than Cloud) project funded by the New Energy and Industrial Development Organization of Japan.

References

- Aki, K. and P. G. Richards (1980). *Quantitative Seismology. Theory and Methods. Vol. 1, 2.* Freeman and Company, San Francisco.
- Barton, C. A. , M.D. Zoback, and D. Moos (1995). Fluid flow along potentially active faults in crystalline rock, *Geology* **23**, 683-686.
- Bresee J.C. (1991). *Geothermal Science and Technology: European HDR Project at Soultz-sous-Forêts.* Gordon and Brech Science Publishers.
- Brown, S. R. (1995), Simple mathematical model of a rough fracture, *J. Geophys. Res.* **100**, 5941-5952, 1995.
- Brune J.N. (1970). Tectonic Stress and the Spectra of seismic Shear Waves from Earthquakes. *J. Geophys. Res.* **75**, 4997-5009.
- Engineering Computer Graphics Laboratory (ECGL) 1996. GMS 2.1. Brigham Young University, Utah.
- Fehler M., L. House, and H. Kaieda (1987). Determining Planes along which Earthquakes occur: method and Application to Earthquakes accompanying hydraulic Fracturing. *J. Geoph. Res.* **92**, 9407-9414.
- Fehler, M. (1989). Stress control of seismicity patterns observed during hydraulic fracturing experiments at the Fenton Hill Hot Dry Rock geothermal energy site, New Mexico, *Int. J. Rock Mech. Mining Sciences and Geomech Abstr.* **26**, 211-219.
- Fehler M. (1990). Identifying the Plane of Slip for a Fault Plane solution from Clustering of Locations of nearby Earthquakes., *Geophys. Res. Lett.* **17**, 969-972.
- Fehler, M. and W. S. Phillips (1991). Simultaneous inversion for Q and source parameters of microearthquakes accompanying hydraulic fracturing in granitic rock, *Bull. Seism. Soc. Am.* **81**, 553-575.
- Hohn, M.E. (1988). *Geostatistics and Petroleum Geology.* Van Nostrand Reinhold, New York.
- Isaaks E.H., and R. M. Srivastava (1989). *Applied Geostatistics*, Oxford University Press, New York.
- Jones R.H., and R. C. Stewart (1997). A method for determining significant structures in a cloud of earthquakes, *J. Geophys. Res.* **102**, 8245-8254.
- Journel A. G., and Ch. J. Huijbregts (1978). *Mining Geostatistics* Academic Press, London.
- Jupe A. J. (1990). Induced Microseismicity and the mechanical Behaviour of jointed Rock during the Development of an HDR geothermal Reservoir. Ph.D. Thesis, Camborne School of Mines, Cornwall.
- Phillips, W.S., L. House, and M. Fehler, (1997). Detailed joint structure in a geothermal reservoir from studies of induced microearthquake clusters, *J. Geophys. Res.* , **102**, 11745-11763.
- Roff A., W.S. Phillips and D. W. Brown (1996). Joint Structures Determined by Clustering Microearthquakes Using Waveform Amplitude Ratios. *International Journal of rock Mechanics and Mining Sciences and Geomechanics Abstracts* **33**, 627-639.

Table 1. Information derived from spatial analysis of data from four zones in the Soultz Hot Dry Rock Reservoir.

Zone	Depth Range (m)	Variogram Function Type	Nugget μm^2	Sill μm^2	Range m	Flow %	Anisotropy Ratio
1	2900-2925	Spherical	0	14000	12	40	2.1
2	2925-2975	Gaussian	8500	4500	16	10	1.1
3	2975-3140	Gaussian	0	8200	12	30	2.5
4	3140-3250	Gaussian	3500	6000	9	15	1.2

Figure Captions

Figure 1. Event distribution within 50 m of injection wellbore GPK1, which is located at West=0. The region is divided into four horizontal slices each having a thickness of 60 m measured in the North-South direction. Injection test of September 1993.

Figure 2. a). Map of contoured variogram function of permeability calculated in directions from 0° degree to 180° (when horizontal axis is given to be 0°). Vertical axes: h_y , horizontal axes h_x . b). Map of relative concentration of tracer. Injection point located in the lower middle of the diagram.

Figure 3. More random pattern of permeability distribution. a). Variogram function of permeability as in Figure 2a. b). Concentration of tracer. Injection location as in Figure 2b.

Figure 4a. Omnidirectional variograms (experimental and model) for zone 1 (depth 2900-2925 m). Labels on experimental variogram indicate the numbers of pairs between events at a specific distance h .

Figure 4b. Omnidirectional variograms (experimental and model) for zone 3 (depth 2975-3140 m).

Figure 4c. Omnidirectional variograms (experimental and model) for zone 4 (depth 3140-3250 m).

Figure 4d. Omnidirectional variograms (experimental and model) for zone 2 (depth 2925-2975 m).

Figure 5a. Directional variogram (experimental and modelled) for zone 3 (2975-3140 m). Direction $90 \pm 15^\circ$. Value a_1 taken for $\gamma(h)=6000$.

Figure 5b. Directional variograms (experimental and modelled) for zone 3 (2975-3140 m). Direction $20 \pm 15^\circ$. Value a_2 taken for $\gamma(h)=6000$.

Peter Starzec
Geology Department
Chalmers University of Technology
412-96 Gothenburg
Sweden
Tel +46317722051
Fax +46317722070
Email: starzec@geo.chalmers.se

Michael Fehler
Los Alamos Seismic Research Center
MS D443
Los Alamos National Laboratory
Los Alamos, NM 87545 USA
Tel 505-667-1925
Fax 505-667-1925
Email fehler@lanl.gov

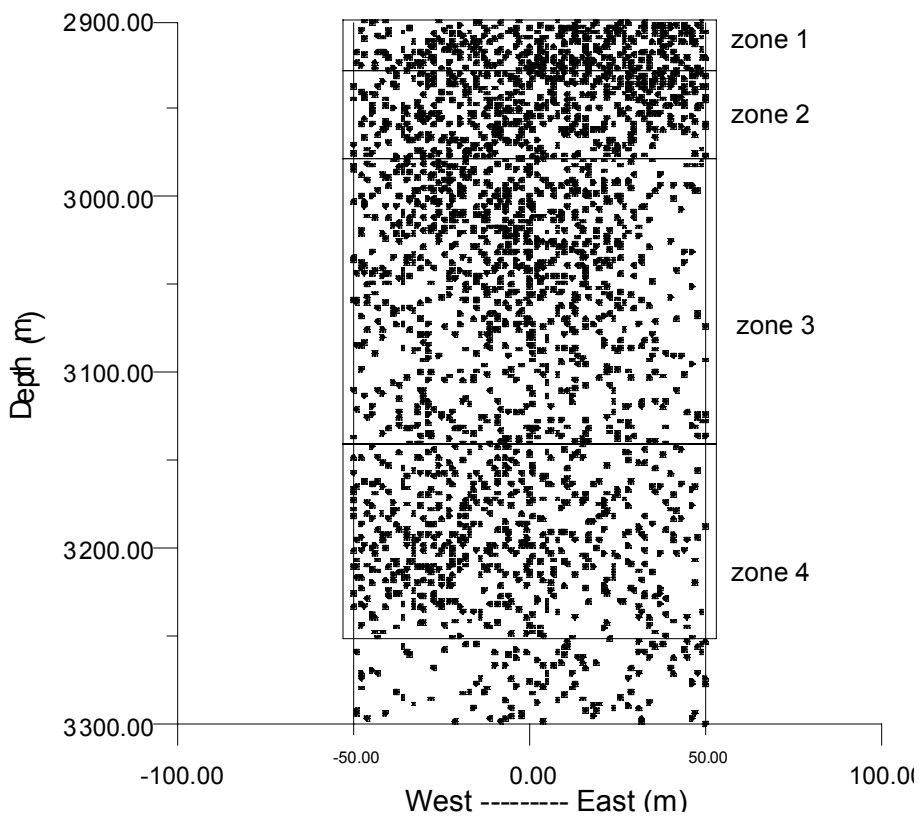
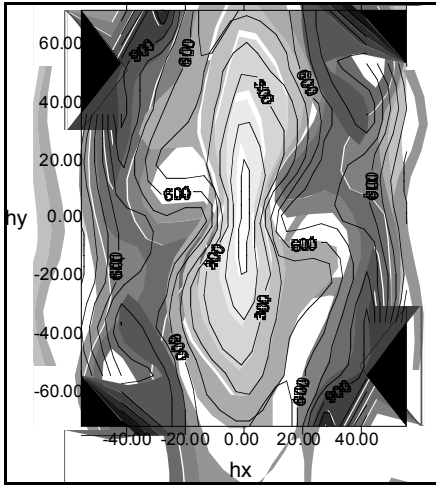


Figure 1.

a



b

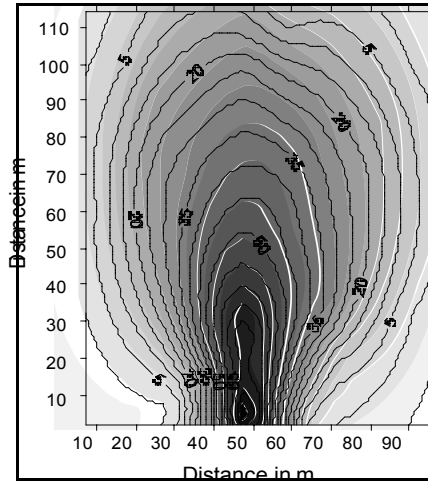


Figure 2.

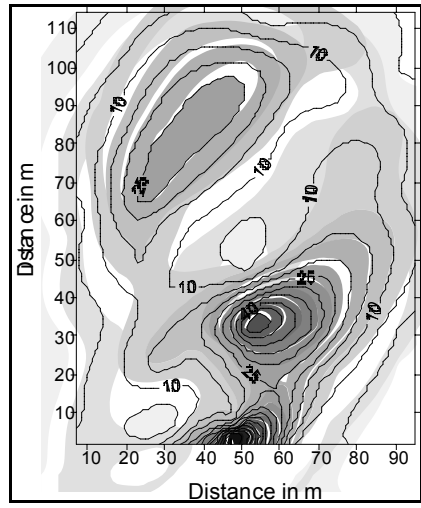
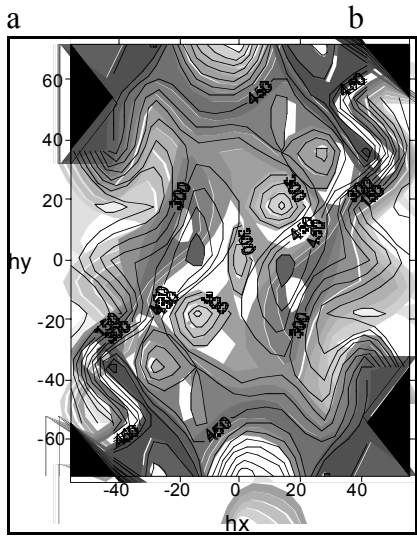


Figure 3

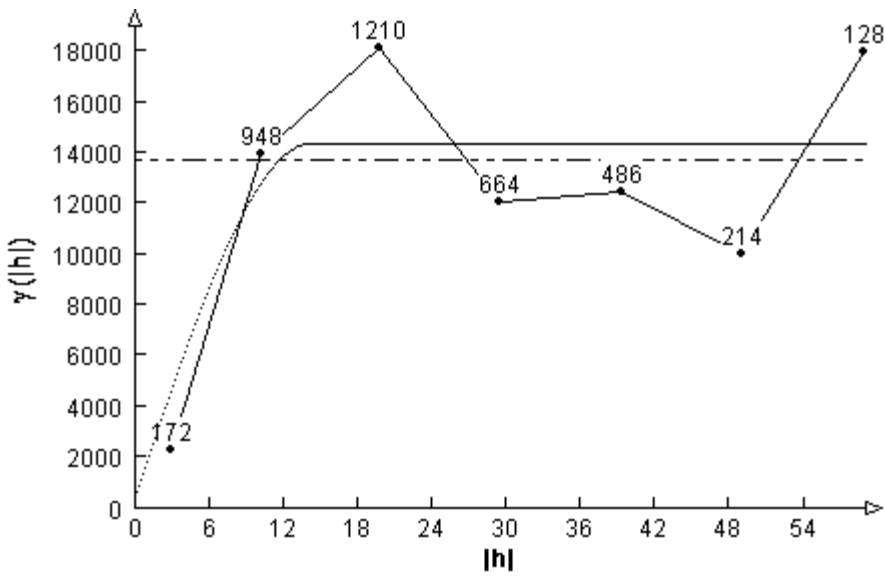


Figure 4a.

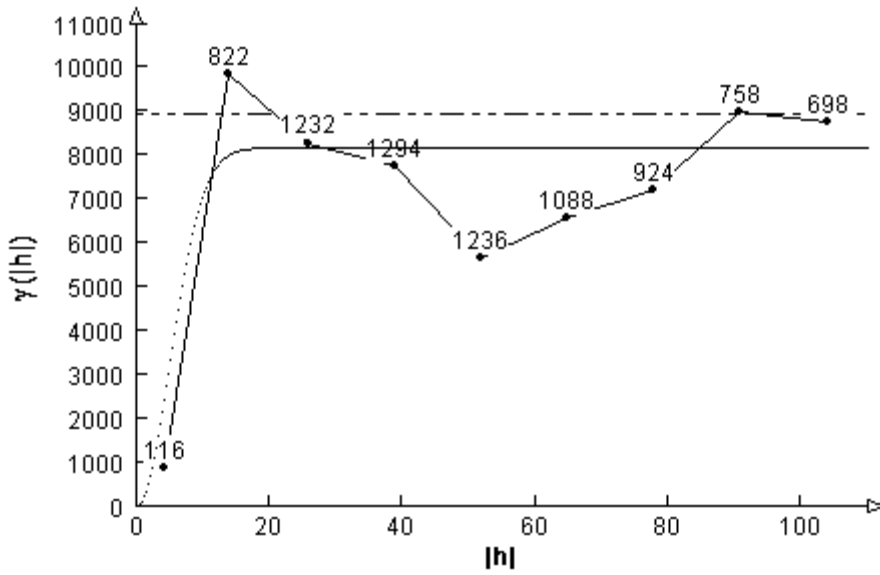


Figure 4b

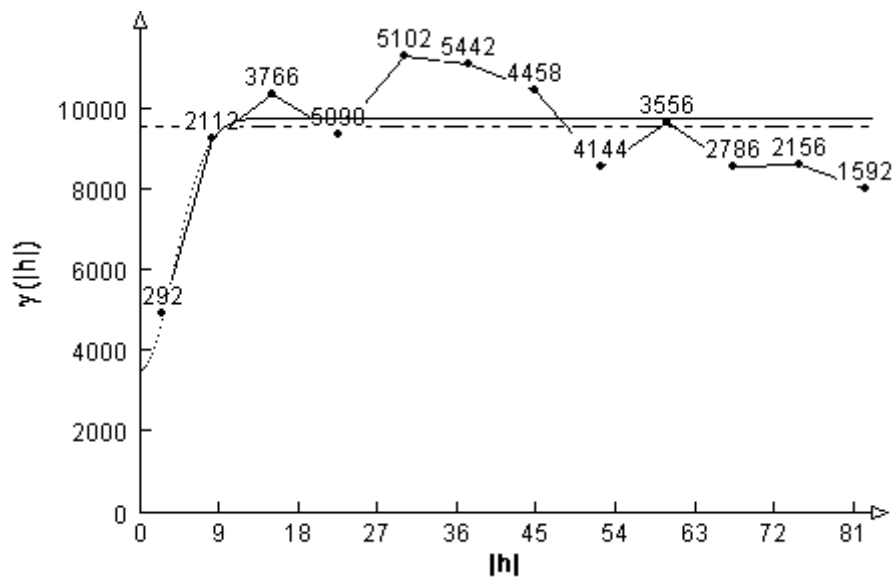


Figure 4c

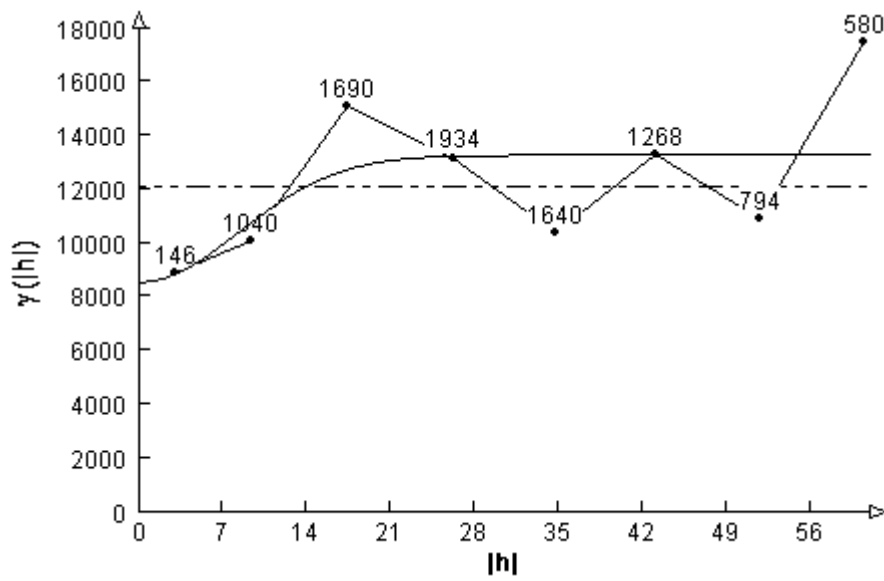


Figure 4d.

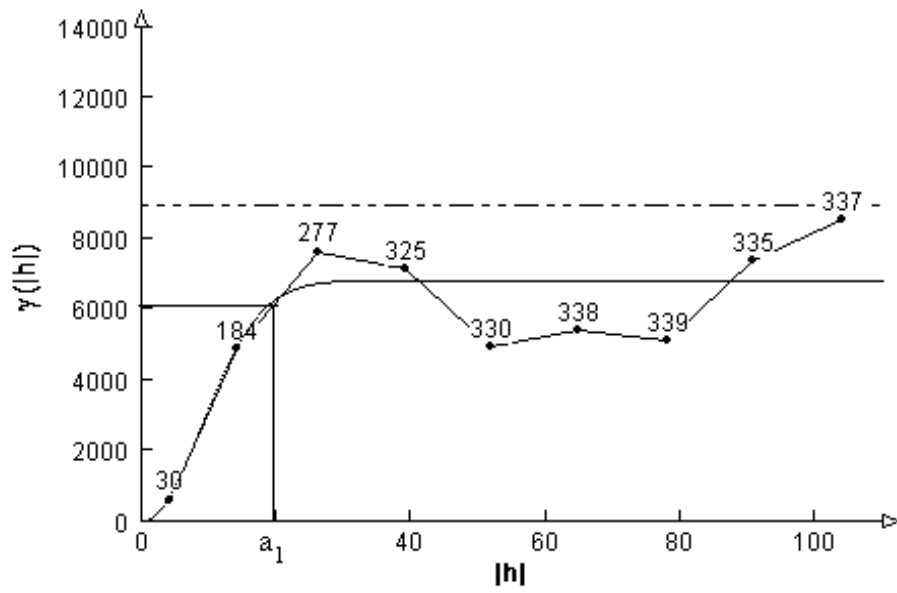


Figure 5a.

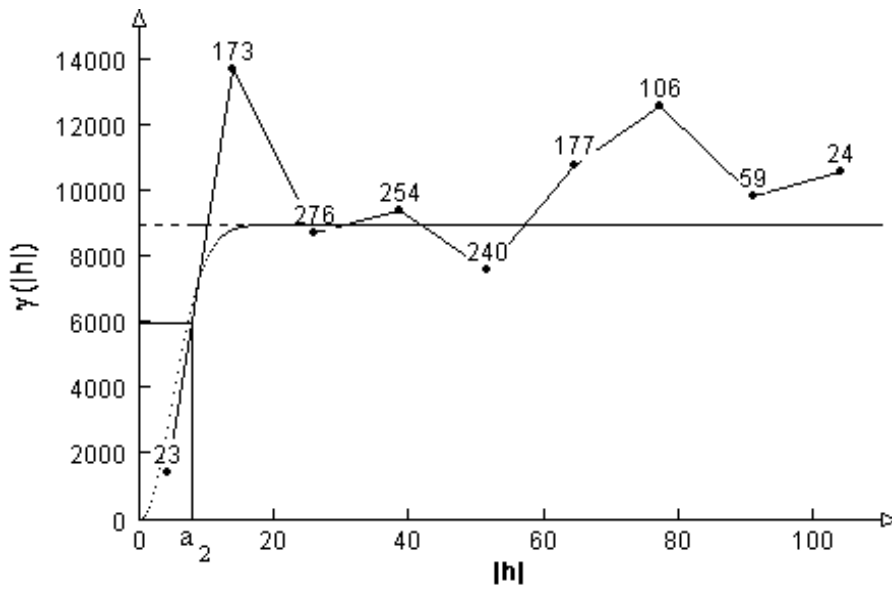


Figure 5b